6-2012

Measuring the Strain Field Gradients on the Surface of a Model Human Skull while Axially Loaded to Simulate Head-loading

Matthew Graveley
Union College - Schenectady, NY

Measuring the Strain Field Gradients on the Surface of a Model Human Skull while Axially Loaded to Simulate Head-loading

By

Matthew Graveley

Advisor: Prof. Jennifer Currey

Union College Department of Bioengineering

March, 2012

ABSTRACT

Measuring the Strain Field Gradients on the Surface of a Model Human Skull while Axially Loaded to Simulate Head-loading

Graveley, Matthew J
Advisor: Currey, Jennifer

Head-loading is a means of transporting heavy loads accross rough, rural terrains practiced by many peoples in Third World countries. Years of practicing head-loading is said to result in increase spinal bone density and permantly grooved skulls [1]. The most infamous people who practice head-loading are the porters of Nepal, who carry loads by means of a head sling straped across their foreheads, and South African women, who carry loads directly on their heads. To simulate and measure the instantaneous micro deformations occurring on the surface of the skull due to head-loading, a test procedure has been developed using a plastic human skull model. The effect of applying an axial load to the skull is examined using a non-contact strain deformation measuring technique known as speckle image photogrammetry. This technique uses two high resolution cameras to monitor the three dimensional deformations occurring on the outer surface of a relatively large portion of the skull. ARAMIS optical deformation software (GOM Optical Measuring Techniques) has been used to compute the strain field gradients on the surface of the model plastic skull while loaded, suggesting a similar test procedure and speckling technique can be used on a masecrated human skull.

I. *Table Of Contents*

II. *Introduction*

Head-loading is the means of transporting goods using ones skull to bear the majority of their weight. For thousands of years, people have used head-loading techniques to carry heavy objects accross rough, rural terrains in the absence of other means of transportation. Today, many people, particularly those who live in developing nations, still rely on head-loading to transport food, water and supplies. Notably, geographic and cultural influences have resulted in different methods of carrying goods. Illustratively, some groups of people, such as the Maasai in East Africa and Porters of Nepal, use a fabric sling straped around the forhead to center loads behind them or on their upper back. Meanwhile, others simply balance loads directly on top of their heads sometimes using small donut-shaped padding to help balance and cushion the load. The Nepalese porters, who use the sling, are world renouned for being able to endure long treks, sometimes for hundreds of kilometres, up and down steep mountain trails [2]. In light of their success, one would assume that the sling technique improves balance and vision, enabling the porters to effectively navigate across mountainous terrain.

In Ghana, Africa, head-loading is predominantly practiced by women who assume the responsibilities of collecting and transporting food, firewood, and water. Meanwhile, boys in Ghana tend to regularly practice head-loading until they are about fifteen years of age. At the young age of three or four, girls have been observed carrying small bowls of water or grain, indicating that head-loading is a highly valued skill. At eight years of age, the girls are said to be able to carry head-loads of approximately 8 kg. Between the ages of fifteen and eighteen, girls are capable of regularly carrying head-loads between 20 to 30 kg or more [3]. In one village in Ghana, both boys and girls carry “large loads” of firewood roughly 10 km to their “district headquarters,” selling the wood prior to attending school. And, in another

village in Ghana, 93% of the students (21 of the 23 surveyed students; aged between 12 to 15 years) claimed they "regularly carried goods for their mothers;" markedly, the two students who did not were both boys [3].

Similarly, another study describing the socio-economic condition of Sub-Saharan Africa, explains that many people in food-growing areas rely on head porterage to bring goods to village markets or road side points accessed by vehicles. More than 90% of the households surveyed in the Ashanti Region, Ghana, claim their principal means of transporting goods out of the field was done by means of head-loading [4]. Specifically, "about 70 percent of agricultural activity [in the Ashanti Region] involves transport with load consignments of 15 to 150 kg carried a distance of 1 to 13 km for on farm trips, and load consignments of 15 kg to 150 kg carried a distance of 1 to 20 kilometers for off farm trips;" head-loads are estimated to average betwen 25 and 40 kg [4]. Again, in the absence of wheel barrows, animals, and vehicles, head-loading is heavily relied upon.

Evidently, several health problems are associated with the head-loading practices, including: backache, head and chest pain, deformation of the spine, and osteoarthritis of soft tissue of the knee. Some health problems associated with head-loading may even have "inter-generational" impacts, resulting in damage to the unborn foetus and miscarriages [3]. Years of this practice is also said to create permanent grooves in head-loaders skulls' [1]. Nevertheless, head-loading remains highly used for reasons being that it is as culturally important as it is a necessity. Despite head-loading's long history and current widespread use, relatively few studies have been conducted to understand how head-loading affects one's physical health.

III. *Background*

The background section is subdivided into the following sections: Comparison of Porterage Techniques, Mechanical Properties of Skull Bones, Anatomy of the Human Skull, and Implications of Form vs. Function. The context of these subsections will help identify the motivation of this project. Few studies are concerned with the implications of head-loading, and little is known about its affects on the skeletal system.

Comparison of Porterage Techniques

Most research dealing with head-loading has been concerned with the relative effecienes of head-loading with respects to back-loading. For instance, some experiments have been designed to test the validty of the "free ride" hypthosis, which states that African women can carry up to 20% of their body mass while head-loading without incurring any extra energy cost [5]. One pilot investigation conducted by Lloyd et al. tested the 'free ride' hypothesis with the help of twenty-four Xhosha women from South Africa; thriteen of which had at least 10 years experience of head-load porterage ("EXP head") and eleven with noprior experience ("NON head"). The women were obeserved walking on a treadmill with head-loads and back-loads between 10% and 70% of their body mass. A a plastic crate (placed either directly on the head or on a small piece of rolled cloth for cussion) was used to apply head-loads, and a standard 45-L backpack was used to apply back-loads. Load-carriage economies were calculated with respects to each loading condition using the extra load index formual, defined as: the ration between loaded oxygen consuption, relative to total load, divided by the unloaded oxygen consumption, relative to body mass. Statistical analysis revealed no significant difference in the relative economy scores of head-loading and back-

loading economy across all loads ($p = 0.206$, 1.04 ± 0.19 for head-loading, and 0.97 ± 0.15 for back-loading). Also, there was no significant difference between the "expert" head and back-loaders, and the "non-expert" head and back-loaders across all loads ($p = 0.186$, ELI $=0.98 \pm 0.17$ for "experts" and 1.04 ± 0.18 for "non-experts") or betweent the different loads ($p = 0.891$, ELI = 1.00 ± 0.16, 1.00 ± 0.17, 1.01 ± 0.18, and 1.00 ± 0.20 for 10%, 15%, 20%, and 25% loads, respectively). Yet, there was a significant difference ($p = 0.015$) between the maximum load carried during head and back-loading (head-loading: $42.1 \pm 14\%$ of BM; back-loading: $51.5 \pm 15.8\%$ BM). Overall, nine of the 24 participants had lower average ELI values for head-loading than back-loading; only 38.5% of the experienced head-loadiers exhibited better economy in head-loading than back-loading. Overall there was a large variability in the ELI data collected in all groups. Although it would be possible to select a subset of women who did achieve high levels of economy while head-loading, the overal findings suggests that the "free ride" hypothesis is not generally true. Ultimately, the ELIs associated with head-loading and back-loading are relatively close in magnitude.

Another experiment concerned with the relative efficiency of head-loading studied Nepalese porters. To do so, researches observed porters carrying goods to sell in a bazaar held in the town of Namche. Many of the porters arrived in Namche after a 7 to 9 day journey from the Kathmandu Valley (covering ~100 km horizontal distance; ~8000 m ascent; ~6300 m descent) [6]. The researchers counted 545 male and 97 female porters (and 32 yaks), and randomly weighted 96 male and 17 female porters. On avererage, the men carried a greater percent of their body mass than the women (men = $93 \pm 36\%$ body mass; women = $66 \pm 21\%$ body mass). Impressively, the greatest load measured was 183% of the porters body mass. To determine the energy cost of porterage while loaded and unloaded, eight Nepalese porters walked around a 51-m flat track at five different speeds while carrying six or seven different loads to collect weight and speed specific respiration data. Weight-specific

metabolic costs were calculated by dividing the energetic cost (ratio of oxygen consumed to carbon dioxide produced) of the loaded subjects by the total mass of their goods and body (similarly, unloaded subjects energetic cost divided by body mass). The Nepalese porters' average weight-specific metabolic costs were compared to that of a control group, European backpackers. The weight-specific cost of carrying for both groups was lowest at the speed of ~1.1 m/s. Comparitively, Nepalese porters had lower weight-specific energy costs than the European backpackers at all speeds and loads: the porters' weight-specific energy cost increased from 0 J kg^{-1} m^{-1} to ~3 J kg^{-1} m^{-1} as loads increased from 15% to 100% of their body weight, whereas the controls' weight-specific enenergy cost was always greater than 3 J kg^{-1} m^{-1}. Similarly, the porters' metabolic power expenditures (oxygen consuption loaded divided by oxygen consumption rate) were calculated with respects to body and load masses, and compared to both the metabolic power expendiure of European backpackers and African women head-loaders measured in previous studies. Conclusively, the Nepalese porters' are more economical than the European backpackers at all loads, and more economical than the African head-loaders at all loads except the lightest loads. Loads lighter than ~20% of the porters' body were considered to be carried for 'free,' meaning the metabolic cost induced by these light loads was characteristic of walking while carrying no load.

Meanwhile, many studies have been conducted to test the effects of loading on bone mass densities. Clearly, bones maintain 'normal' stress levels with respects to average loads transmitted by either absorbing or producing bone matrix as needed. In light of these observations, one study tested the correlation between bone mass densities (BMD) and head-loading in thirty-two black, South African women (22.4 ± 3.2 years). Of the thirty-two women, eighteen were considered load carriers, or head-loaders, and fourteen were non load carriers, or non head-loaders. Ten of the women (six load carriers and four non load carriers) used injectable progestin contraception (IPC) for birth control. IPC prevents ovulation by

reducing the pulse frequency of gonadotropin-releasing hormone, which reduces the secretion of follicle-stimulating hormone, preventing an increase in oestradiol. Consequentially, limiting oestradiol may affect bone metabolism and cause bone loss [7]. The subjects' loading histories were qualitatively obtained via interviews, and their total body, lumbar spine and total hip BMD were measured via dual energy X-ray absorptiometry. When excluding the IPC users, the data obtained from these methods demonstrated that there was a correlation between the average weight of the load carried and the lumbar spine BMD ($r = 0.743$, $p < 0.005$); and, also between years of head-loading and lumbar spine and total body BMD ($r = 0.563$, $r -= 0.538$, respectively; both $p < 0.005$) [7]. Conclusively, head-loading may offer osteogenic benefits to the spine, if not the whole body. However, benefits do not appear to extend to women using IPC, suggesting that loading alone cannot sufficiently counteract hormonal influences. Further studies should be conducted to increase the population sample size.

Mechanical Properties of Skull Bones

Other studies have been conducted to determine the mechanical properties of the skull bones. Even though these studies are not directly related to head-loading, the data collected can be used to help calculate how the skull transmits loads. In particular, one study tested the mechanical properties of cranial bone samples taken from the skulls of embalmed cadavers who were individuals ranging between 56 and 73 years at their time of death. The study determined that the material properties of the embalmed bone were not significantly different from the properties of living bone. Notably, the structural arrangement of the diploë, the spongy bony structure of the internal part of flat bones, caused large variations in the data collected. Despite bone's complex structure, the researchers considered the bone to be homogeneous for reasons of simplicity. Ultimately, they deduced that the cranial bones'

modulus is proportional to the third power of density, while the bones' strength is proportional to the fourth power of density. Thus, if the porosity of bones with low relative density slightly changes, then only small changes in strength and modulus will occur. Yet, if the porosity of bones with high relative density slightly changes, then large changes in strength and modulus occur [8]. Although their results do not directly demonstrate how the skull responds to loads applied to the head, the data collected by this study could be vital to developing models representative of the human skull transmitting loads characteristic of head-loading. Ultimately, because there are few reports related to head-loading, my aim is to present information relevant to creating a reasonable test procedure designed to measure the strain gradients on the surface of the skull while axially loaded. Afterall, one can't help but to wonder how head-loading inmpacts bone remodeling and skeletal development — especially in young African girls.

Anatomy of the Human Skull:

For the purpose of biomechanics, the human skull lies beneath the connective tissue of the scalp and above the durra mater which surround the brain and cerebral spinal fluid. The skull bones are composed of three layers, where the outer and inner cortical bone layers surround a dipole layer. As opposed to the inner and outer rigid bone surfaces, comparable to that of the corticies of vertebral and long bones, the inner dipole is soft and compositionally similar to the cancellous bone of the human vertebral column. Despite having symmetrical properties about the mid-sagital plane, the cranial vault is rather complex [9]. Furthermore, the adult skull bone can be divided into the frontal, top (vertex), rear (occipital), and side regions. The side of the skull is divided into the parietal (superior) and temporal (inferior) regions (Figure 1). Each skull bone has unique shape and thickness properties. The temporal region is thinner in comparison to the parietal, occipital and frontal regions. The parietal

region is convex outwards while the temporal region is concave. Due to distinctive variations in geometric shape and thickness, the characterization of the effects of head-loading on independent regions of the skull is difficult to predict.

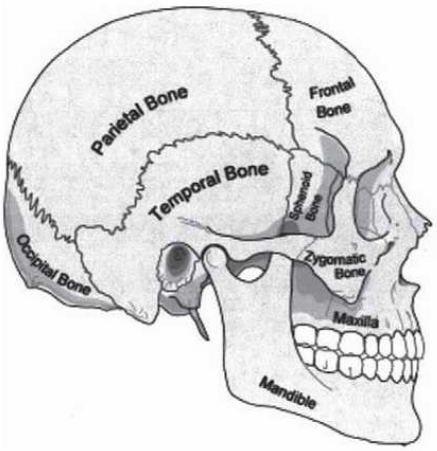

Figure 1: Later view of the skull showing the bones that makeup the human skull [9].

Furthermore, precise mechanisms ensure that the morphology and rate of bone growth parallel that of the brain development. During early stages of development, the skull is composed of plates that form into different regions with cartilaginous components acting as connecting elements. The newborn skull is about 4% as stiff as an adult skull, yet it quickly undergoes maturation to attain about 75% stiffness between the years of 6 and 8 [9]. The cartilaginous components, the fontanels, of the skull coalesce with age. And, unlike most bones affiliated with age related osteoporosis, the skull bones do not predominantly demonstrate this type of strength loss due to having relatively larger portion of cortical regions [9].

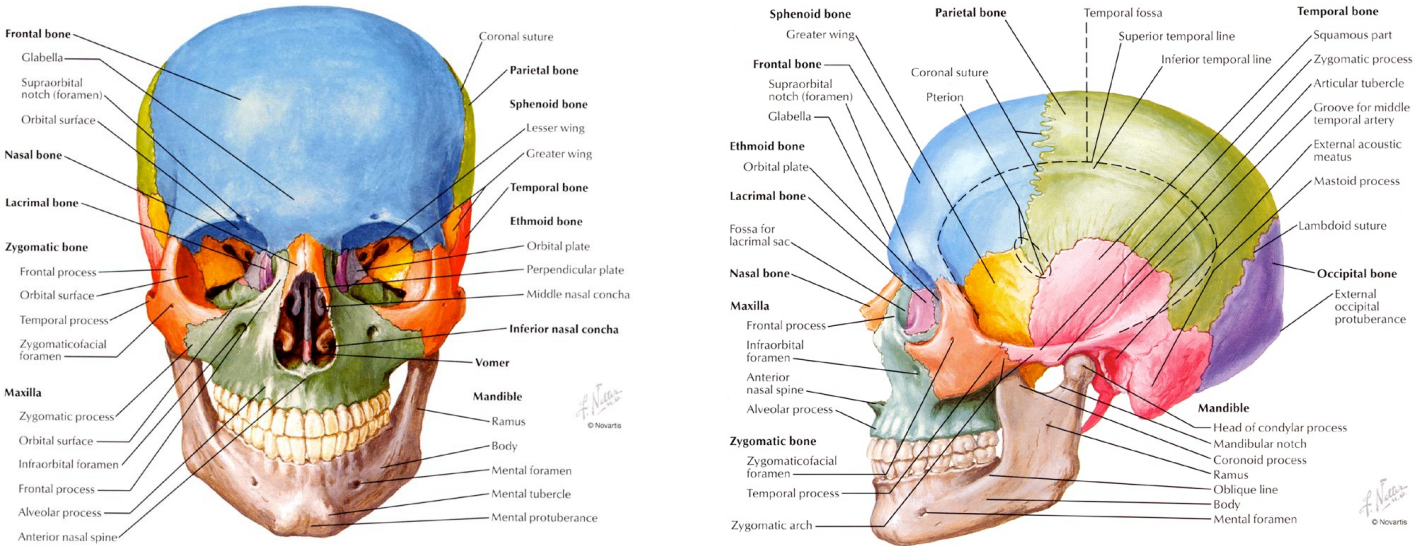

Figure 2: Frontal and lateral view of the bones of the skull [10].

The cervical region of the spine is greatly valued for its role in providing the head with structural support and functional mobility. The cervical spine is composed of seven vertebrae, which are linked in series from the base of the cranium to the upper end of the thoracic spine; the upper most vertebra being C1 and lowest being C7. Between each adjacent vertebra is a disc that acts as the shock absorbing cushioning that permits some movement between the bones. Strong fibers, called longitudinal ligaments, run along the cervical spine to provide the neck with greater structural support. Several finite element analyses of the cervical spine have been made to supplement our understanding of the spinal network's structural response to different loading conditions. Data suggests that neck ligaments and muscles respond to loading, causing the human cervical spine increases in stiffness when higher loads are transmitted through the neck [9]. These findings will be beneficial to explaining the role of the cervical spine in distributing external loads induced by head-loading.

Implications of Form vs. Function

The human skull plays a role in a variety of critical functions such as cognition, vocalization, respiration, diet, and thermo regulation. Its unusual craniofacial apomorhies make "humans the only extant primate with an external nose, without a snout, a spherically shaped (globular) braincase, a highly flexed cranial base, a face that is retracted almost entirely beneath the braincase, fur on just the top of the head, a chin, and so on" [11]. Its unique shape may prompt you to ask, why is the human skull designed the way it is? Or, how are its characteristics advantageous to its role in the human system? And, how is its form, shape, and function interrelated? The purpose of this section is to briefly discuss recent hypotheses relating the human skull's form to its evolutionary function—neurocranial sphericity, facial shortening and retraction contributed to cognition, mastication, locomotion, respiration, and speech. Noticeably, the skull's evolution has little to do with its ability to bear weight.

***Cognition*:** It was once thought that the human skull's shape supported the development of a relatively larger frontal lobe. However, comparative studies in hominoids disproved this hypothesis; in fact, when proportionally scaled, the frontal, parietal, and occipital lobes in humans are about the same relative size as in other hominoids. Presently another attractive hypothesis states that the relative increases in the temporal lobe of the brain played a role in the evolution of the humans – no further evidence has supported or disproved this hypothesis [11].

***Mastication*:** In light of having relatively shorter faces than other primates, the human craniofacial shape was not selected to increase masticatory efficiency. Since humans have small and thinly enamelled tooth crowns that have become smaller, humans produce relatively low bite forces with respects to our body size. This is partly due to the reduction in the cross-sectional area of some muscles, which are also composed of relatively fewer fast

twitch muscle fibres. One hypothesis is that *Homo sapiens'* dietary intake gradually changed from a limited range of raw tough foods to a broader range of cooked dietary rich softer foods. As food preparation and cooking techniques have developed, there is a reduced need for large teeth and jaw size [11].

Locomotion: Even though the skull's shape is less commonly related to locomotion, it has been hypothesized that the decreases in facial size have benefited head stabilization while running. Identifiably, humans have features not present in apes that assist with head stabilization. For instance, the human head has more "sensitive anterior and posterior semicircular canals" to sense accelerations, and a "nuchal ligament, which may act as a passive, elastic mechanism to stabilize the head." Finally, the human head is anatomically balanced on top of the cervical vertebrae to reduce the moment arm experienced by the neck [11].

Respiration and thermoregulation: Smaller faces also have been explained to be functionally beneficial in the role of respiration and thermoregulation because the superior-inferior and anterior-posterior shorting decreases the length of the pharyngeal airway. During normal activities, breathing out of the nose, the nasopharynx, creates turbulent airflow, "increasing the efficiency of the respiratory epithelium, especially for recovering moisture." And, during "vigorous activity," the switch to oral breathing benefits from the shortened oral cavity which helps "improve the efficiency with which we dump head" [11].

Speech: Not to say that 'archaic humans couldn't speak,' but based on the observations that both the modern humans' have a shorter oral cavity (by at least a centimetre) and more flexed cranial base ('decreasing the pharyngeal space behind the plate by another centimetre'), some hypothesize that inherited craniofacial morphologies enabled

modern humans to produce ‘more quantal vowels that would be more stable and less susceptible to errors of perception’ [11].

Ultimately, despite protecting the soft tissues of the brain, the human skull’s form does not appear fit for bearing external loads inflicted by head-loading techniques. Since it is well known that bone remodelling takes place in presence, or absence, of stress, I would like to understand how the skull transmits axial loads to predict how the human skull would change as result of practicing head-loading. Further knowledge of head-loaders’ general health may also provide insight into more specific skeletomusclar responses induced by head-loading—particularly, those in the head and neck.

Purpose of Head-loading Study

Ultimately, my aim is to create a test model that places human masecrated skulls in a loading enviornment similar to that induced by techniques of head-loading. Using Specle Image Photogrammy, the deformation of the skull induced by loading will be calculated into strain field gradients. This method requires the use of two high resolution cameras and ARAMIS software (GOM Optical Measuring Techniques). ARAMIS software will digitize the video, taken of the skull while loaded, into photographs, and trace the displacements of the speckle pattern applied to the surface of the skull. The speckled pattern will be made by spraying a light coat of spraypaint to the surface of the skull. The displacements of each speckle with respects to its initial position are used to create vectors needed to calculate relative strains, producing images indicative of strain fields [12]. The data will be used to better understand how strains are trasmitted throughought the geometrically complex shapes that compose the skull. The locations with greatest strain concentrations may correspond to the areas where indentation has been observed to occur as result of years of head-loading.

IV. *Materials and Methods*

The Materials and Methods section is broken down into two subsections: Equipment and Test Procedure. The Equipment section will focus on the ARAMIS Photogrammetry system, model skull, and load frame, meanwhile the Procedure section will describe the speckle pattern technique, camera calibration, and data collection. The following test proceedure designed to induce axial loading and measure surface deformations is relatively straight forward, yet time comsuming. The Procedure section of this report is written to enable the reader to easily duplicate the experiment, which resulted in sufficient preliminary strain data.

Equipment

ARAMIS Photogrammetry System

Speckle image photogrammetry was used to mesure the strain induced on the surface of the skull. The ARAMIS 2M Photogrammetry System (GOM Optical Measuring Techniques, Mittleweg 7-8, 38106 Braunschweig, Germany) was used measure the material properties as the model humn skull with cervical vertebrae was axially compressed. The ARAMIS software coupled with the 2M camera system was used to measure the displacements in the x and y-axes and compute the major and minor surface strain values undergone by the model skull via tracking a speckle pattern. The 2M system's two syncronized cameras, with 50 mm lenses, are used to capture still images of the skull as it undergoes compression (Figure 3). ARAMIS's computational software measures and calculates the displacements of the speckles with respects to the images caputured by the two cameras. In this proceedure, the speckle pattern was created using white Color Place matte spray paint for a non-reflective base layer, and black Model Master matte spray paint for the speckles.

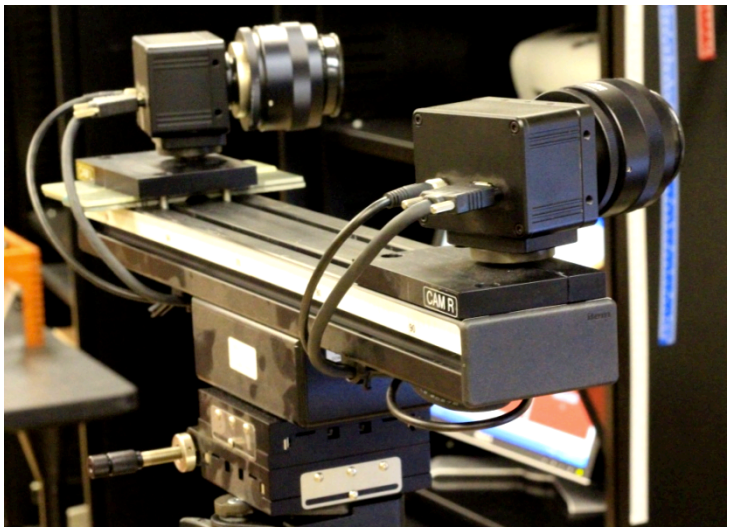

Figure 3: The ARAMIS 2M's two cameras equipted with 50 mm lenses, base distance of 400 mm, and camera angles of 30˚.

To focus the cameras on the surface of the model skull, the cameras are positioned at a set distance away from its exterior surface ("measuring distance") so that their focal points intersect. The measuring distance between the skull and the cameras is dependent on a number of variables such as the type of camera lenses used, the angle of the cameras with respects to one another, and the distance between of the cameras ("base distance"). In this test procedure, the base distance between the cameras was 400 cm and the angle of the cameras respects to one another was approxiately 30˚. The base distance and cameara angle produced an appropriately sized field of view with a substantial depth of field to measure surface strain of a section of the parietal and frontal bones while under compression.

Once the cameras are positioned to produce the desired field of view, the cameras need to undergo a standard calibration proceedure. The proceedure requires the use of a calibraton pannel that has an adequate volume with respects to the desired field of view, or measuring volume. To calibrate the 2M system, the CP 20 calibration plate made by GOM Optical Measuring Techniques (Mittleweg 7-8, 38106 Braunschweig, Germany) was used (Figure 4). The pattern on the surface of this panel has coded and uncoded reference points which enables the software to accurately track pixel movement as the panel is repositioned

throughout the calibration process. After the system has been calibrated, it is important not to touch the cameras or tripod, because small vibrations or alterations of the physical system will result in measurment errors.

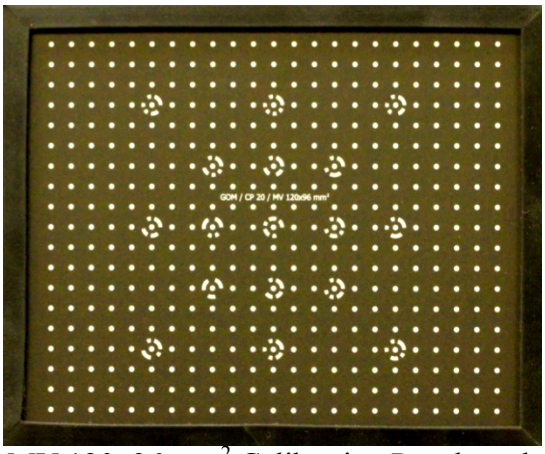

Figure 4: GOM/CP 20/ MV 120x96 mm^2 Calibration Panel used to calibrate the cameras.

The calibration process also requires the calibration plate to be well lit, yet glare free, to enable the cameras capture images with quick shutter speeds (shutter time ≈ 13-18 ms). Two heat lamps, each euqiped with dimmers (Magic Gadgets 2K Pro Inline Dimmer, Aurora, Oragon), were used to porperly light the calibration panel and model skull. Although there was no glare on the CP 20 calibration pannels due to the surface properties of the CP 20 pannel, there was glare on the surface of the model skull after applying the initial speckle pattern. Fortunately, simple measures were taken (applying a white spray paint for base of black speckled paint) to alter the inital speckle pattern on the surface of the skull, reducing the glare that inhibited the ARAMIS system from measuring speckle displacements.

The Model Skull

The model skull used in this test proceedure is the "Budget Skull w/ Cervical Vertebrae" manufactured by Anatomical Chart Company in China (Figure 5). Accordingly, the models made in China are made of a relatively low quality PVC type of plastic. The skull

model is also said to be casted using another plastic skeleton model, and not from the original human skelton, reducing its anatomical accuracy and quality [14]. Regardless of the model's relatively low grade quality, the skull was chosen for the purpose of designing the experimental procedure. This model was also chosen because it consists of 7 cervical vertebrae, nerve branches, and vertebral arteries which are center mounted on a steel threaded bolt. In this proceedure, the bolt which projects through the cervical vertebrae's verebral foramen, was used to mount the model skull to the base of the compression cage. The bolt helps to prevent the cervical spine from bending, yet does not inhibit the vertebrae from compresing.

Figure 5: PVC Human Model Skull: "Budget Skull w/ Cervical Vertebrae" (size: 8-1/4" W x 11-1/4" H x 8-1/4" D) mounted in the compression cage.

Load Cell Equipted with Compression Cage

A 20,000 lbs capacity load frame (Model TTD 78"/22"- Instru-Met Corporation, Union, NJ) was used to apply an axial compressive load to the skull while mounted in the compression cage (Figure 6). The model skull was threaded into to the hole on the base of the compression cage using the threaded bolt which intersects the model's vertebral foramen and a female to male threaded adapter. The compression cage converts the tensile load produced by the load frame into a compressive load. TestWorks software (Software

Research Inc., San Francisco, CA) was run on a computer connected to the load frame to operate the load frame, controling the magnitude of force applied.

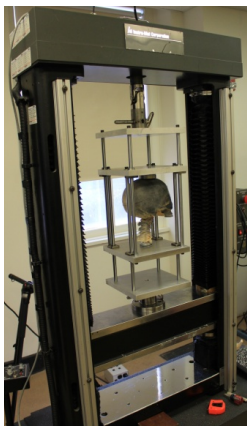

Figure 6: Photograph of the load frame (Model TTD 78”/22”- Instru-Met Corporation, Union, NJ), compression cage, and mounted model skull.

An aluminum casting cup placed on the top of the skull to help transmit the load from the flat surface of the compression cage onto the convex apex of the skull. The casting cup was manufactured out of multipurpose aluminum (Alloy 6061, 2-1/2" Diameter, 1" Long), and bismuth casting alloy, or “woods metal,” (158-190 Degree F Melting Temperature) was used to create a rigid mold of the skull’s irregular surface (Figure 7).

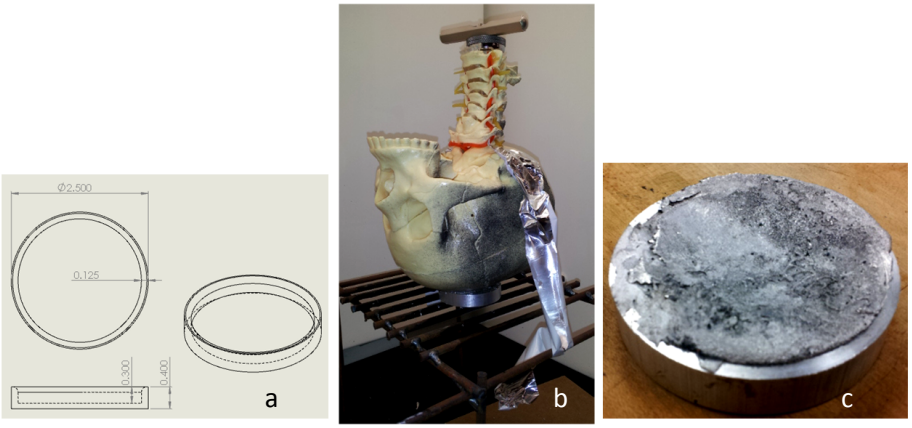

Figure 7: a) dimensional drawing of casting cup b) skull positioned on top of casting cup to mold the bismuth alloy while it cooled - An air bubble level is placed on the spacer washers to help align mold c) photo of molded bismuth alloy inside aluminum casting cup - bismuth alloy was melted using a propane torch.

Test Proceedure

Speckel Pattern

Several speckle patterns were tested using plain white paper and two types of black spray paint. Both types of spray paints were applied to sheets of paper using the following different techniques: horizontal spray strokes, vertical spray strokes, and spurts of sprays. Each technique was applied to the white paper at various distance intervals ranging from approximately 12 cm to 30 cm. The resulting patterns were compared to GOM's ARAMIS Spray Pattern Reference pattern applied to a 100 x 80 mm sheet to help determine which technique resulted in a viable speckle pattern. Color Place's spray was too fine to use even when sprayed a short distance away from the paper. The best pattern resulted when vertically spraying Model Master 's black matte spray paint at approximately 23 cm away from the surface of the paper. The quality of pattern was verified based on the ARAMIS software's ability to recognize the high contrast, approriately sized speckle pattern. To reduce the reflective glare of the model skull's PVC surface, a coat of Color Place's white matte spray paint was added to the skull before applying the layer Model Master's black spray paint.

Camera Calibration

Before each trial measurement, the ARAMIS 2M camera system must be calibrated according to a standard thirteen step proceedure. This proceedure tends to be time consuming and requires attention to detail. For this procedure, a field view of 120 x 96 mm^2 was chosen based on the availability of the CP 20 calibration panel. The CP 20 calibration pannel surface is made of ceramic, making it vulnerable to touch and is easily damaged by finger prints (Figure 4). Hence, it is important to avoid touching the surface of the panel during calibiration, and the panel must be properly stored in it's protective casing after its use. Luckily, the 120 x 96 mm^2 field of view volume is large enough to sufficiently measure

a large portion of the model skull's parietal bone and some of its neighboring frontal and temporal bones.

Prior to calibration, the two 50 mm camera lenses must be properly positioned so that the cameras focal points intersect at the same spot on the calibration panel (the center coded reference point) on the surface of the calibration panel. Because the base distance between the cameras (400 cm) and the camera angles (30˚) are ideal for measuring the desired field of view, the calibrator must position the camera tripod so that the cameras' focal points intersect at same spot on the calibration panel. For this specific procedure, the placement of the calibration panel is extremely important; specifically, the surface of the calibration panel needs to be positioned in the exact plane in which the skull's surface of interest will be located post calibration (Figure 7). In other words, the the placement of the calibration panel during calibration must compare to the placement of the external surface of the model skull when it is fixed in the compression cage. Again, the camera tripod must be accurately placed prior to calibration, because any adjustment to the camera system post calibration will result in error.

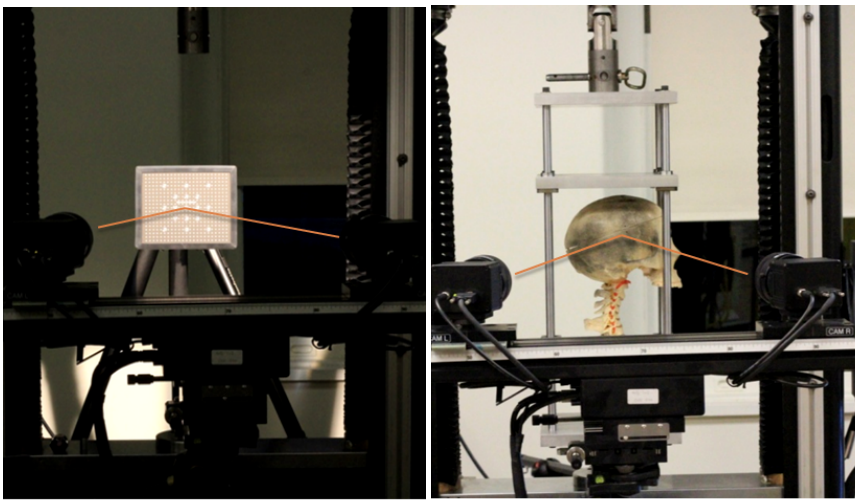

Figure 7: Positioning of the calibration panel with respects to the outer surface of the model skull. Lines represent the convergence of focal point at same point on the surface of the object.

After the calibration panel and camer tripode were properly positoned, the lenses were focused. To do so, the lenses aperatures were phyiscally opened all the way, over exposing the images, and then the shutter speed was decreased using the ARAMIS software until very little of the image was over exposed. Then, both the the lenses were physically focused to increase the clairty of the images. Thereafter, the the lenses aperatures were phyically closed all the way, and the ARAMIS software was used again to increase their shutter speeds until the images were were well lit, and not overexposed. The calibration panel was mounted on a tripod, allowing it to be repositioned as specified throughout the calibration proceedure (Figure 6). To initiate the calibrtion procedure, select the calibration mode in the ARAMIS software. This mode provides instructions to guide the calibrator through a 13 step procedure, in which the calibrator move and rotates the calibration plate using the appropriately design tripod (Figure 8). More informtion about the calibration proceedure can be found in the GOM ARAMIS V6 User Manual [14].

Figure 8: Calibration Panel mounted to tripod with horizontal sliding arm.

Given the previously descriped ARAMIS 2M camera system setup, the actual actual measuring volume on the surface of the skull was approximately 90 x 74 mm (Figure 9). This measuring volume was adequate, but should be increased during future experimentation. The data collected during the experiment was done while the skull was placed under a set of compressive loads with increasing increments of 5 lbs, starting at 10 lbs and ending at 25 lbs. The maximum load of 25 lbs was applied to prevent the model PVC skull from breaking or

perminantly deforming. A complete view of the test setup, with the important equipment components labeled, can be seen in Figure 10.

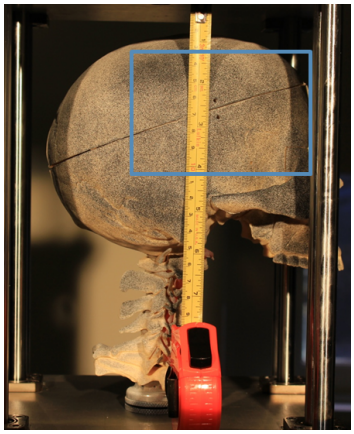

Figure 9: Rectangle on surface of skull represents the approximate measuruing volume (90 x 74 mm) using ARAMIS 2M camera system.

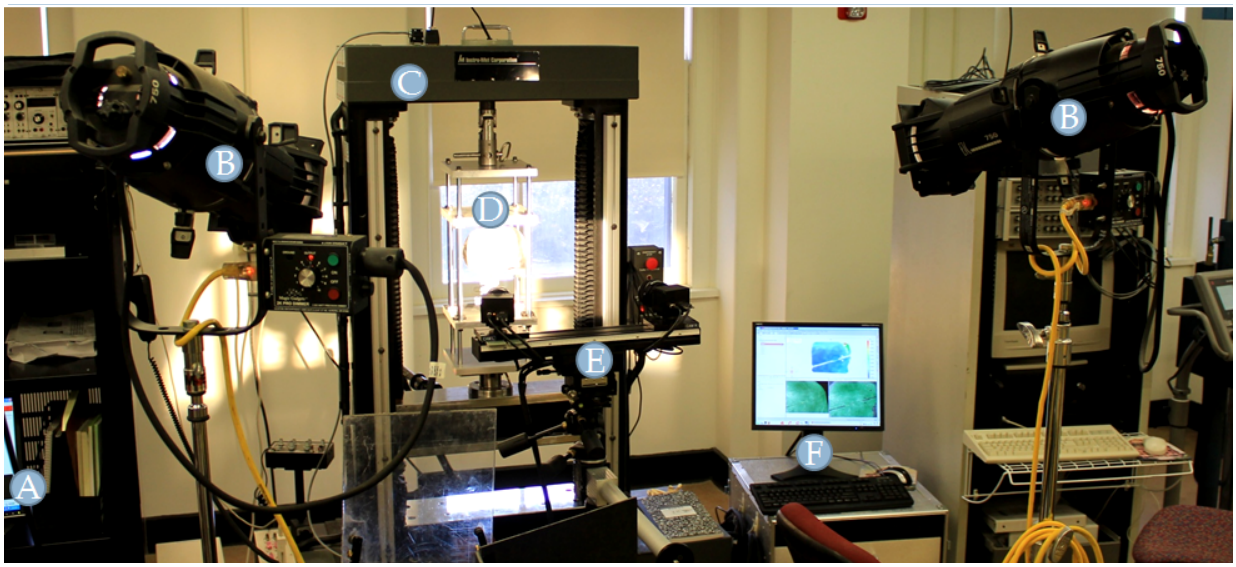

Figure 10: A) Computer with TestWorks software for operating load cell, B) Heat Lamps – ETC, Source Four equipped w/ damping adjustablility, C) Load Frame – Instru-Met Corporation, Model TTD 78"/22" (Capacity 20,000 lbs), D) Compression cage and mounted skull w/ vertebrae, E) ARAMIS 2M system – two cameras w/ 50 mm lenses, F) Computer with ARAMIS Software for displacement and strain computations

V. *Preliminary Results*

The preliminary data collected verified the experimental setup and procedure can be followed to measure displacement and compute strain data. Each set of 6 images correspond to the following compressive loads: a) Reference Image (0 lbs), b) 0 lbs, c) 10 lbs, d) 15 lbs, e) 20 lbs, and f) 25 lbs. First, the sequence of x-axis displacement images suggests the skull rotated because the displacement gradients are the greatest on the right most portion of the image. Intuitively, these results make sense because the load was transmitted through the aluminium casting cup placed on the frontal, and left and right parietal bones, creating a moment about the cervical spine. Second, the y-displacement images similarly suggest the skull was rotating because the vertical displacement gradients greatly shift when viewing the image from left to right. Third, both the minor strain and major strain sequence of images suggest the skull underwent the greatest deformation on the top of the skull, suggesting the strains are highly concentrated around the aluminium casting cup.

Furthermore, the data may also suggest that there is potential for the system to erroneously calculate displacement and strain information due to the curvature of the skull. In other words, the depth of field of the 50 mm lenses may be too shallow to accurately track speckle patterns on the convex surface of the skull. For example, take a look at the major strain field gradients occurring on the frontal bone (most upper right portion of each strain image) under each loading condition (Figure 14); noticeably, the maximum major strain concentration calculated when 0 lbs was applied was 0.120%, increasing to 0.200% when 25 lbs was applied (Table 1). Observationally, this portion of the model skull is greatly curved, and distant from the plane in which the camera system was calibrated to measure in.

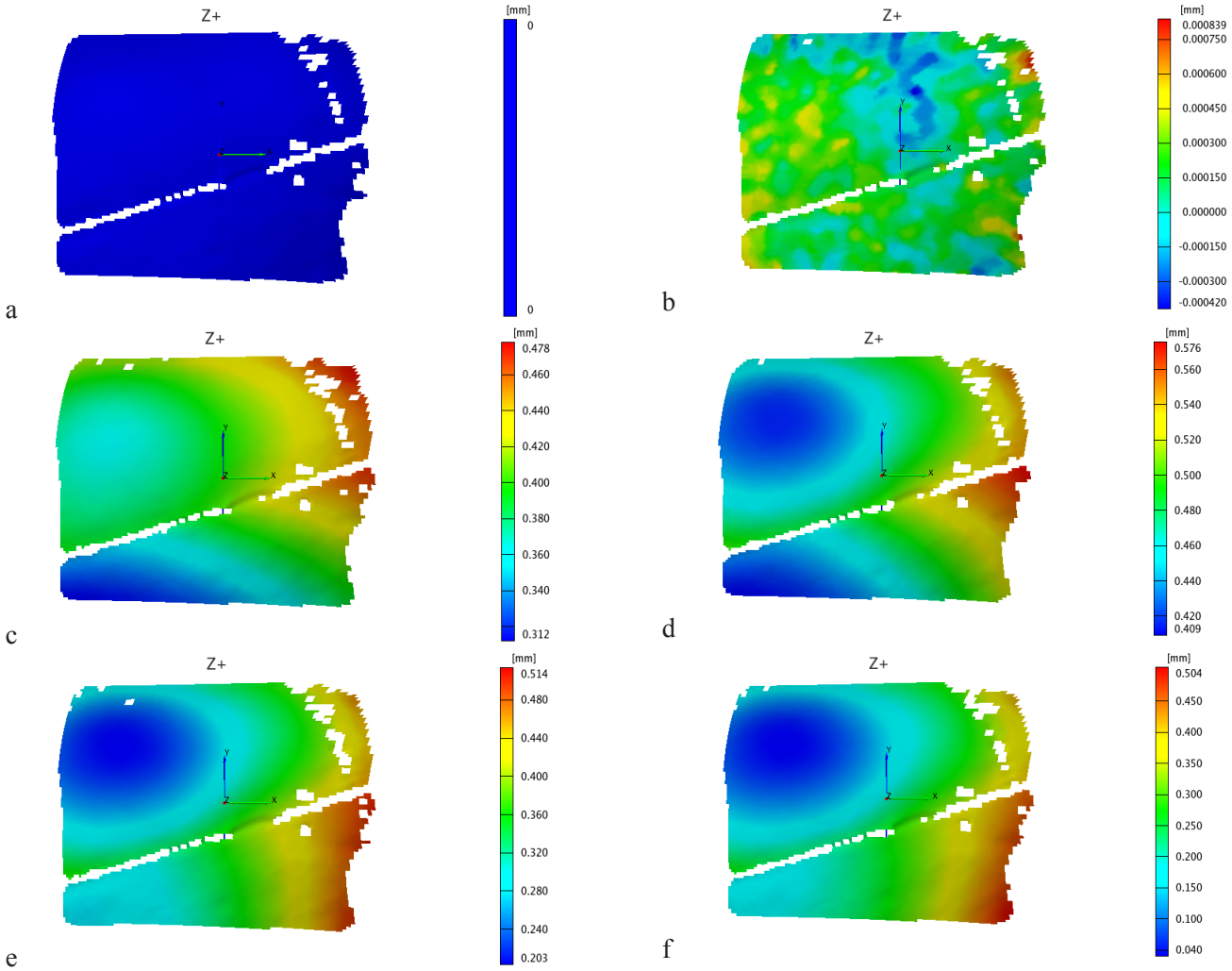

Figure 11: Displacement gradients in the x-axis : a) Stage 0: 0lbs b) Stage 1: 0 lbs c) Stage 2: 10 lbs d) Stage 3: 15 lbs e) Stage 4: 20 lbs e) Stage 5: 25 lbs

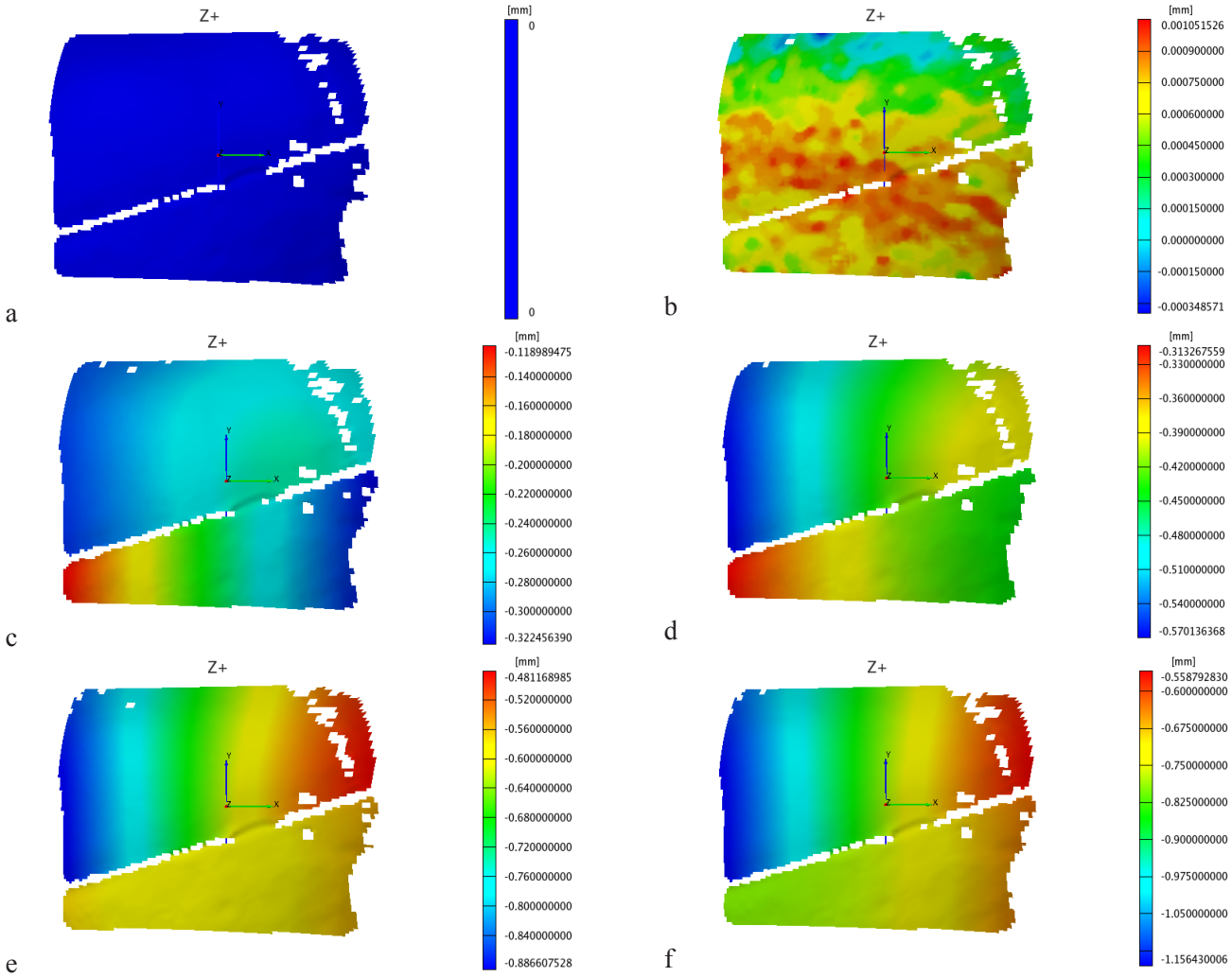

Figure 12: Displacement gradients in the y-axis a) Stage 0: 0lbs b) Stage 1: 0 lbs c) Stage 2: 10 lbs d) Stage 3: 15 lbs e) Stage 4: 20 lbs e) Stage 5: 25 lbs

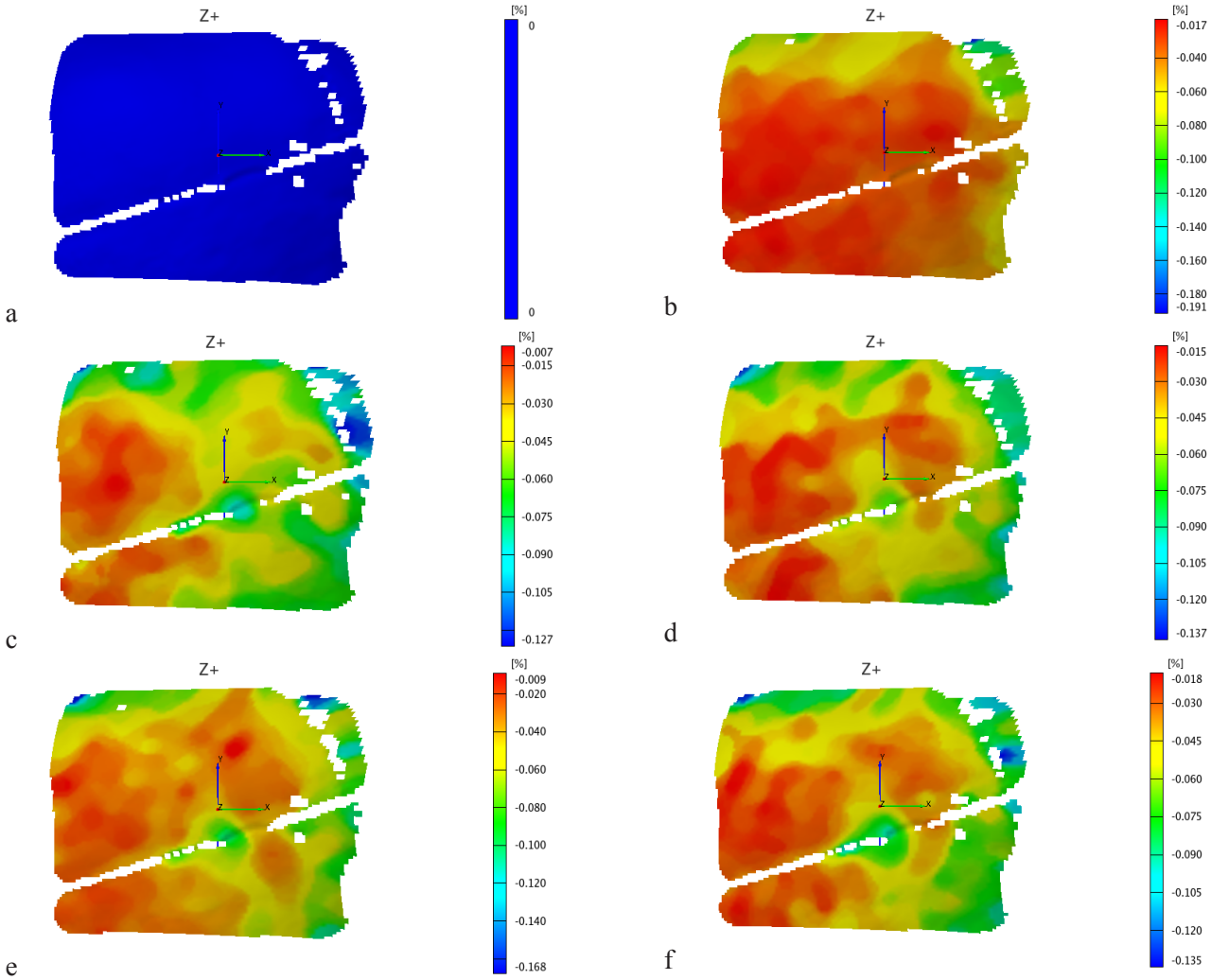

Figure 13: Minor strain field gradients a) Stage 0: 0lbs b) Stage 1: 0 lbs c) Stage 2: 10 lbs d) Stage 3: 15 lbs e) Stage 4: 20 lbs e) Stage 5: 25 lbs

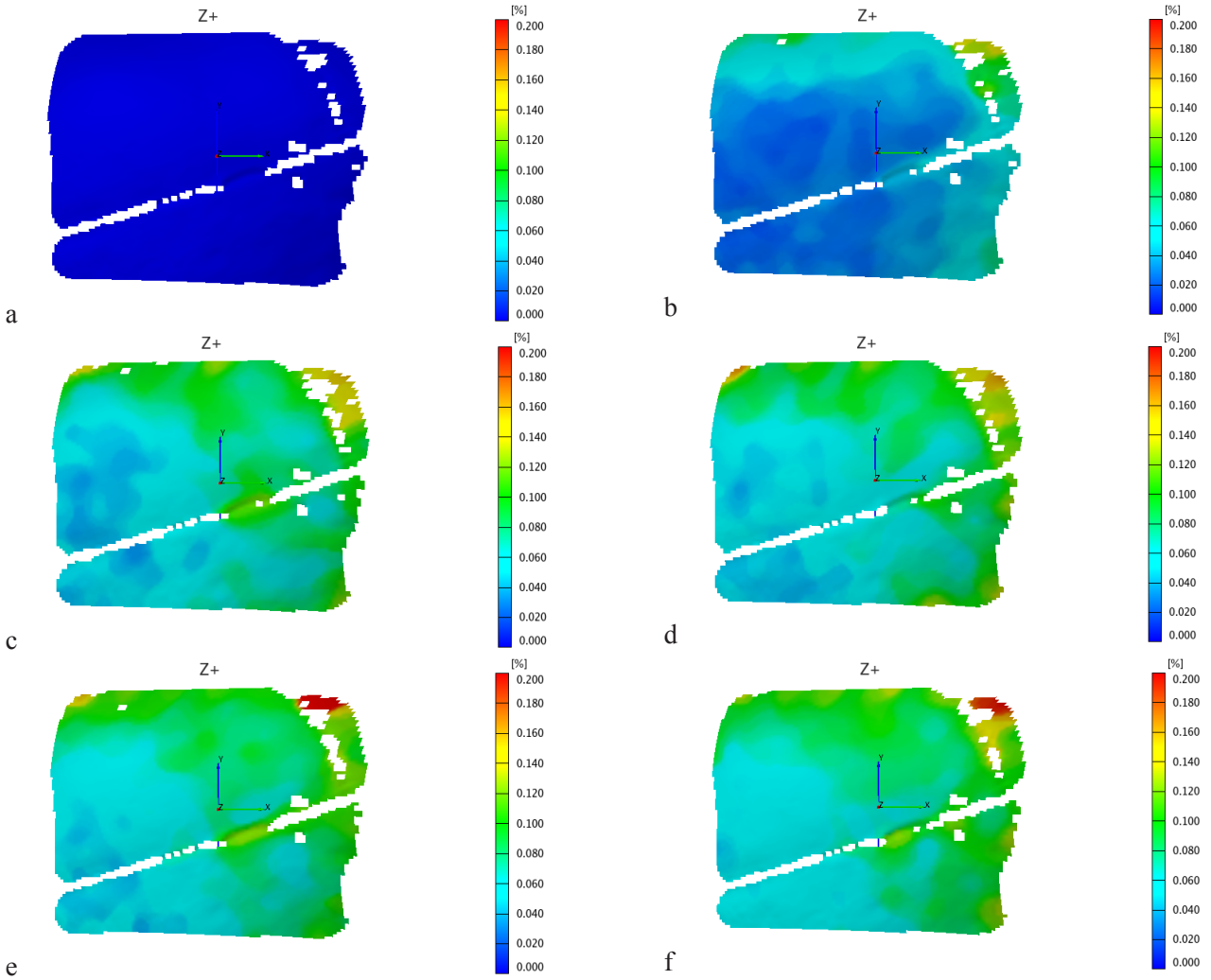

Figure 14: Major strain field gradients a) Stage 0: 0lbs b) Stage 1: 0 lbs c) Stage 2: 10 lbs d) Stage 3: 15 lbs e) Stage 4: 20 lbs e) Stage 5: 25 lbs

Table 1: Table comparing the maximum values displacements in the x and y-axes, and minor and major strains the model skull experienced while axially loaded.

Applied Load	Max ΔY displacement (mm)	Max ΔX displacement (mm)	Max Δ Minor Strain (%)	Max Δ Major Strain (%)
0	0.000839	-0.00035	-0.120	0.120
10	0.478	-0.32246	-0.127	0.130
15	0.576	-0.57014	-0.137	0.180
20	0.514	-0.88661	-0.168	0.200
25	0.504	-1.15640	-0.135	0.200
Overall Δ	0.503	-1.15605	-0.015	0.09

VI. *Discussion and Conclusion*

The procedure designed to measure the surface strains on the external surface of the model skull produced usable results. The model skull chosen, although anatomically flawed and made of low grade PVC, was adequate for testing the experimental procedure. Notably, the cervical vertebrae appeared to undergo the greatest amount of displacement in the y-axis as the compressive load increased. This observation was expected because the ventral and dorsal surfaces of the vertebrae are surrounded by silicon-like nerve branches and arteries. However, interestingly, this observation also correlates with the fact that cervical vertebrae are believed to increase in bone mineral density as result of practicing head-loading.

Markedly, a significant amount of time was spent becoming familiar with the ARMIS 2M photogrammetry system and learning how to perform calibration procedures with respects to the objects of interest. Due to this time demanding phase, only one set of displacement and strain data was collected.

Future Research

In the future, it will be important to obtain a real human skull with cervical vertebrae to perform the experiment. Using a real skull will create new challenges, one of which would deal with the means of adequately stabilizing vertebrae and skull in the testing environment. Or perhaps a bolt, similar to the one used in the current model, could be used to align the cervical spine without inhibiting the vertebrae from compressing. And perhaps a thin layer of silicon glue could be used to pad the ventral and dorsal sides of each vertebra to further stabilize the spine.

Furthermore, the currently used aluminium casting cup should be either modified or replaced with cloth padding. Ideally, a spherical-seat platen should be manufactured to help reduce the amount of bending induced by the currently used aluminium woods metal cup (Figure 15). More research should also be conducted outside of this study to further understand the qualitative and quantitative correlations between strain and bone formation. Ultimately, this test procedure is still in its early design phase and has the potential to be greatly modified and improved upon.

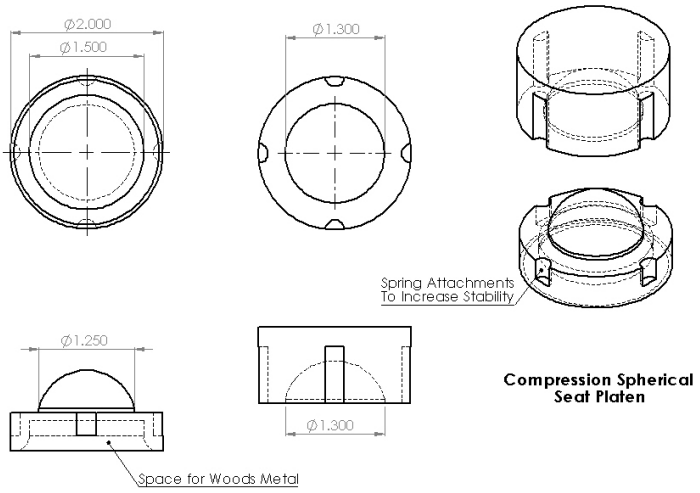

Figure 15: Proposed drawing of a Compression Spherical-Seat Platen designed to ensure loads are transmitted through the y-axis, potentially reducing the bending moment about the spine. The design is based on a product manufactured by Wyoming Test Fixtures, Inc.

References

1) Dweck, Jessica. “Head Case: The Art and Science of Carrying Things on your Head.” Slate Online Magazine, August 27th, 2010.

2) Ebert, Jessica. “Nepalese porters bear up best: African women pipped to the post for most efficient portering.” BioEd Online. June 16, 2005.

3) Porter, Gina, Blaufuss, Kathrin, and Acheampong, Frank Owusu (2004). “Youth, mobility and rural livelihoods in sub-Saharan Africa: perspectives from Ghana and Nigeria.” University of Durham.

4) Riverson, John D. N., and Carapetis, Steve. “Inermediate Means of Transport in Sub-Saharan Afria.” World Bank Technical Paper Number 161 Africa Technical Department Series. 1991.

5) Llyod, Ray, Parr, Bridget, Davies, Simeon, Cooke, Carlton (2009). “No ‘Free Ride’ for African Women: A Comparison of Head-Loading versus Back-Loading among Xhosa Women.” South African Journal of Science, 106.

6) Guillaume J. Bastien, Be´ne´dicte Schepens, Patrick A. Willems, Norman C. Heglund (2005). “Energetics of Load Carrying in Nepalese Porters.” Science, 308: 1755.

7) Llyod, Ray, Hind, Karen, Micklesfield, Lisa K., Carrol, Sean, Truscott, John G., Parr, Bridget, Davies, Simoene, and Cooke, Carlton (2010). “A pilot investigation of load-carrying on the head and bone mineral density in premenopausal, black African women.” Journal of Bone Mineral Metabolism, 28: 185-190.

8) McElhaney, James H., Fogle, John L., Melvin, John W., Haynes, Russell R., Roberts, Verne L., and Alem, Nabih M. (1970). “Mechanical Properties of Cranial Bone.” Journal of Biomechanics, 3: 495-511.

9) Yoganandan, Narayan, and Pintar, Frank A. (2004). “Biomechanics of temporo-parietal skull fracture.” Clinical Biomechanics, 19:225-239.

10) Netter, F.H. *Atlas of Human Anatomy* (1997). East Hanover, New Jersey: Novartis.

11) Teo, E.C., Ng, H.W (2001). “Evaluation of the role of ligaments, facets and disc nucleus in lower cervical spine under compression and sagittal moments using finite element method.” Medical Engineering & Physics, 23: 155-164.

12) Lieberman, Daniel E (2008). “Speculations about the Selective Basis for Modern Human Craniofacial Form.” Evolutionary Anthropology 17:55-68.

13) Jian H. Yu and Peter G. Dehmer (2005). “Dynamic Impact Deformation Analysis Using High-speed Cameras and ARAMIS Photogrammetry Software.” Weapons and

Materials Research Directorate, Army Research Laboratory-Aberdeen Proving Ground, MD 21005

14) "Skeleton Models." 2007. Web. <https://www.shopanatomical.com/default.asp>.

15) GOM. “ARAMIS v6 User Manul – Software.” Braunschweig, Germany: 2007.